Research Article
Multivariate Analysis of the Senegalo-Mauritanian Area by Merging Satellite Remote Sensing Ocean Color and SST Observations

[1,3]O. Farikou, [2]S. Sawadogo, [1]A. Niang, [4]J. Brajard, [4]C. Mejia, [4]M. Crépon and [4]S. Thiria
[1]Ecole Supérieure Polytechnique, Université Cheikh Anta Diop (Dakar), BP 5085 Dakar Fann, Sénégal,
[2]Ecole Polytechnique de Thiès, BP A10 Thiès, Sénégal
[3]Institut Universitaire des Sciences et Techniques d'Abéché (IUSTA), Tchad
[4]IPSL/LOCEAN, unité mixte CNRS-IRD-UPMC-MNHN, Case 100, 4 Place Jussieu,
75005 Paris France

Abstract: The Senegalo-Mauritanian upwelling is a very productive upwelling occurring along the West coast of Africa. The seasonal and inter-annual variability of the upwelling region between 9° and 22°N and 14° and 25°W was studied by merging monthly ocean color data and sea surface temperature provided by satellite sensors during twelve years from 1998 up to 2010. We combined these two parameters to obtain a unique index describing the spatio-temporal variability of the upwelling. We used a classification methodology consisting in a neural network topological map and a hierarchical ascendant classification. Six classes can explain most of the variability of this region, one of them (class 6) being dedicated to the coastal upwelling water, another being the signature of the Gulf of Guinea dome water (class 2), a third one to case 2 water (class 5). The classes can be considered as multi-factorial statistical indices allowing us to characterize the different water types of this region and to investigate their variability. It is shown that the upwelling extent is maximum in February-March, minimum in August-September. Its variability is linked to that of the wind and to the ITCZ position. The Gulf of Guinea waters moves northward in June and relaxes to their southward position in December. During the twelve years of observation, we were not able to evidence climatic trends of the SST and Chl-a concentration. The methodology we have developed can be used in a large variety of problems implying multi sensor measurements.

Keywords: Data fusion, machine learning, oceanography, phytoplankton, remote sensing

INTRODUCTION

The Senegalo-Mauritanian upwelling is a very productive coastal region occurring along the West coast of Africa. It extends from 26°N down to 10°N. It has been well documented during the past decades from *in-situ* and satellite observations. For a review of the physics (Barton, Eastern Boundary of the North Atlantic. 1998) and the biogeochemical behavior (Aristegui *et al.*, 2004). The major forcing are the trade winds blowing South-westward, which generate an offshore Ekman transport generating an upwelling of deep cold waters rich in nutriments favorable to phytoplankton development. The analysis of satellite-derived chlorophyll concentration and Sea Surface Temperature (SST) (Lathuiliere *et al.,* 2008) showed that the Senegalo-Mauritanian upwelling can be split into two regions, one north of 21°N (Fig. 1) where the seasonality is very weak, the other south of that latitude, where the upwelling presents a strong seasonality. In the south part, the upwelling intensity is maximum at the beginning of spring (March to April)

showing an offshore SST gradient with cold SST along the coast and high phytoplankton concentration (Fig. 2 and 3). The intense upwelling period is associated with a strong phytoplankton bloom, which extends far away offshore, as shown in ocean color satellite images. It weakens in June and disappears from mid-July to the end of summer, period for which the offshore horizontal SST and chlorophyll concentration gradients decrease (Fig. 2 and 3). The weakening in the upwelling is due to that weakening of the trade winds linked to the Northward displacement of the Inter Tropical Convergence Zone (ITCZ) driving the rainy season. North of 21°N, there is a quasi-permanent upwelling of which the corresponding chlorophyll-*a* concentration extends far offshore associated with filaments and eddies.

In fact, this schematic description is, in reality, much more complicated. The studied area is the eastern termination of the North Atlantic Tropical gyre. It is influenced at its northern boundary by the Canary current (CanC) flowing southward and the North Equatorial Current (NEC) flowing southwestward and
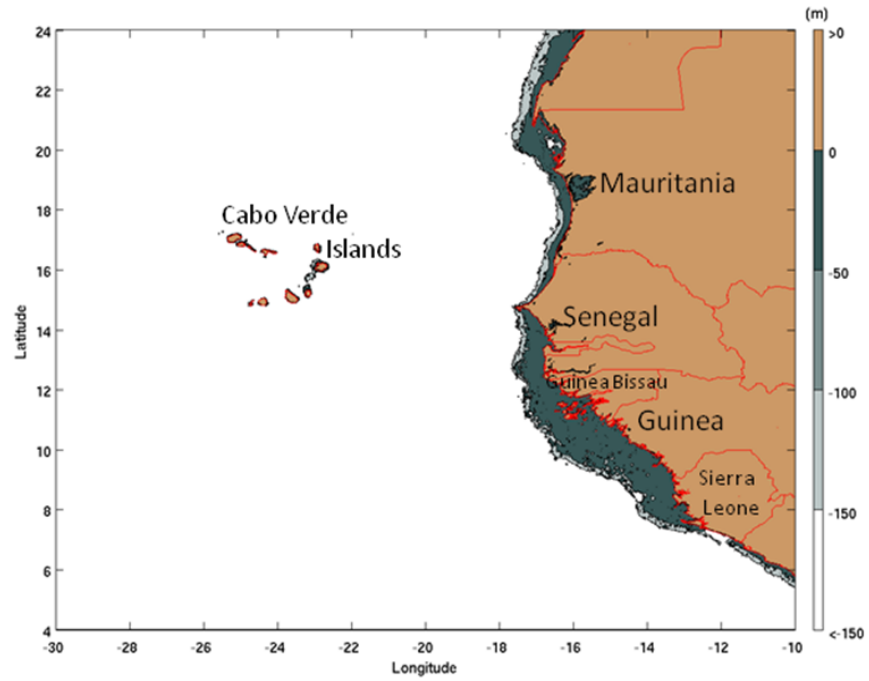
Fig. 1: Mauritania and Senegal coastal topography. The land is in brown and the ocean depth corresponds to the color scale in meters (right side of the figure)
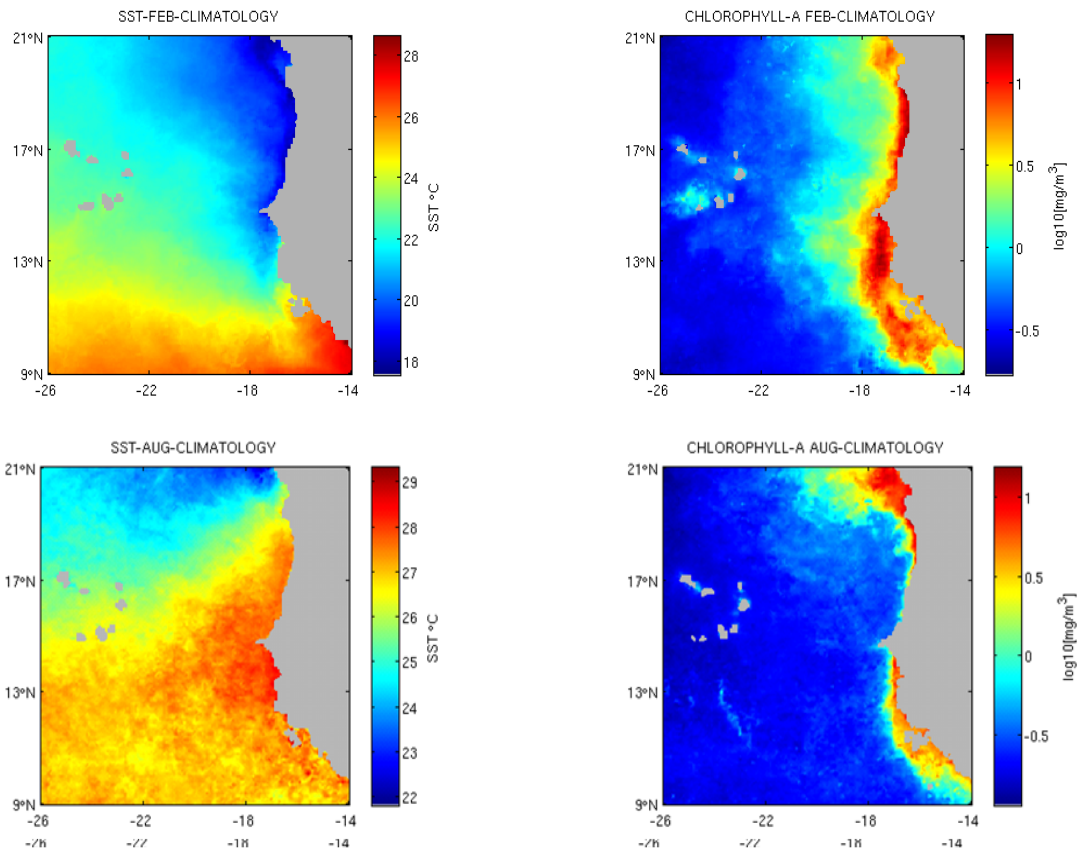

Fig. 2: Climatology of the SST (left panels) and chlorophyll-*a* concentration (right panels) for the months of February (upper panels) and August (lower panels) averaged for the ten years of observation
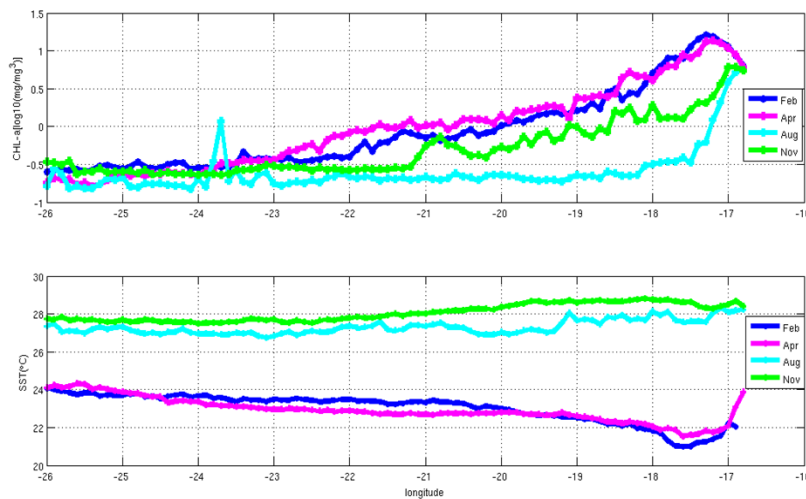
Fig. 3: SST (upper panel) and chlorophyll-*a* (lower panel) zonal sections (February, April, August and November) along 17° N

at its southern boundary by the North Equatorial Counter Current (NECC) flowing eastward. Seasonal fluctuation and meandering of these currents may modulate the upwelling region and the structures and characteristics of the associated waters (Lathuiliere *et al*., 2008).

The aim of the present study is to combine ocean color and SST satellite observation in order to extract optimum information on the upwelling dynamics, in a much more efficient way than the information obtained by processing the two data sets separately. For that, we propose to cluster ocean situations presenting similarities, both with respect to chlorophyll concentration and to SST. For this, we chose a neural network clustering method, i.e., the Self Organizing Map (SOM) (Kohonen, 2001). SOM have been used in many geophysical studies to extract information of huge data set leading to understand complex phenomena. It has recently been applied to study the biological production in eastern boundary upwelling systems by Lachkar and Gruber-(2012).

We focused our interest on monthly time scale due to the necessity to average the satellite images on a sufficient time to remove the effect of clouds, which can prevent the sea surface observation with satellite sensors, especially during the rainy season (July, August and September). At that time scale, SST and Chlorophyll-a concentration (Chl-a in the following) measured by satellite are proxies of the upwelling, SST being a signature of the dynamical behavior of the upwelling whereas Chl-a is a mixed signature of the dynamics and the integrated biological activity. Due to its own dynamics, Chl-a is able to enhance ocean physical structures not revealed by SST. Furthermore, we have processed the normalized ocean color spectra given by the SeaWiFS sensor in order to tentatively retrieve additional information such as the biogeochemical water type (case 2 water) or the phytoplankton species.

THE SENEGALO-MAURITANIAN UPWELLING

Coastal upwelling zones are very productive ocean regions. More than 80% of the ocean productivity is encountered in upwelling regions. The upwelling physical characteristics and behavior have been extensively described in the scientific literature (O'Brien and Hurlburt, 1972; Allen, 1973; Brink, 2005). Coastal upwelling is characterized by vertical motion of deep, hence cooler, water reaching the surface coastal layers. Its offshore extent is of the order of the first baroclinic radius of deformation (some tens of kilometers depending on the location and stratification). Its intensity is related to the along shore wind component which generates an offshore Ekman transport and consequently an upward vertical movement of water at the coast to satisfy the continuity equation. The upwelled water supplies nutriments to the surface layer, thus favoring the blooming of phytoplankton. The pattern of the upwelling is modulated by the alongshore variability of the wind, the coastline geometry (Crepon *et al*., 1984; Beletsky *et al*., 1977), the bottom topography and instabilities of the fluid motion. Schematically, one observes a strip of cold surface water with high chlorophyll concentration parallel to the coast and whose front with offshore surface waters may oscillate (Barth, 1989) and form filaments (Bricaud *et al*., 1987; Lange *et al*., 1998; Lathuiliere *et al*., 2008). The signature of the upwelling is well observed on satellite Sea Surface Temperature (SST) and ocean color images, permitting the analysis of its variability.

In this research, we aimed at extracting the most pertinent information from satellite ocean color observation and SST on the Senegalo-Mauritanian upwelling in order to characterize its variability and the mechanisms driving it. For this, we analyzed 10 years (from 1998 up to 2007) of monthly sea surface chlorophyll concentration (Chl-a in the following) provided by the SeaWiFS (Sea-viewing Wide Field-of
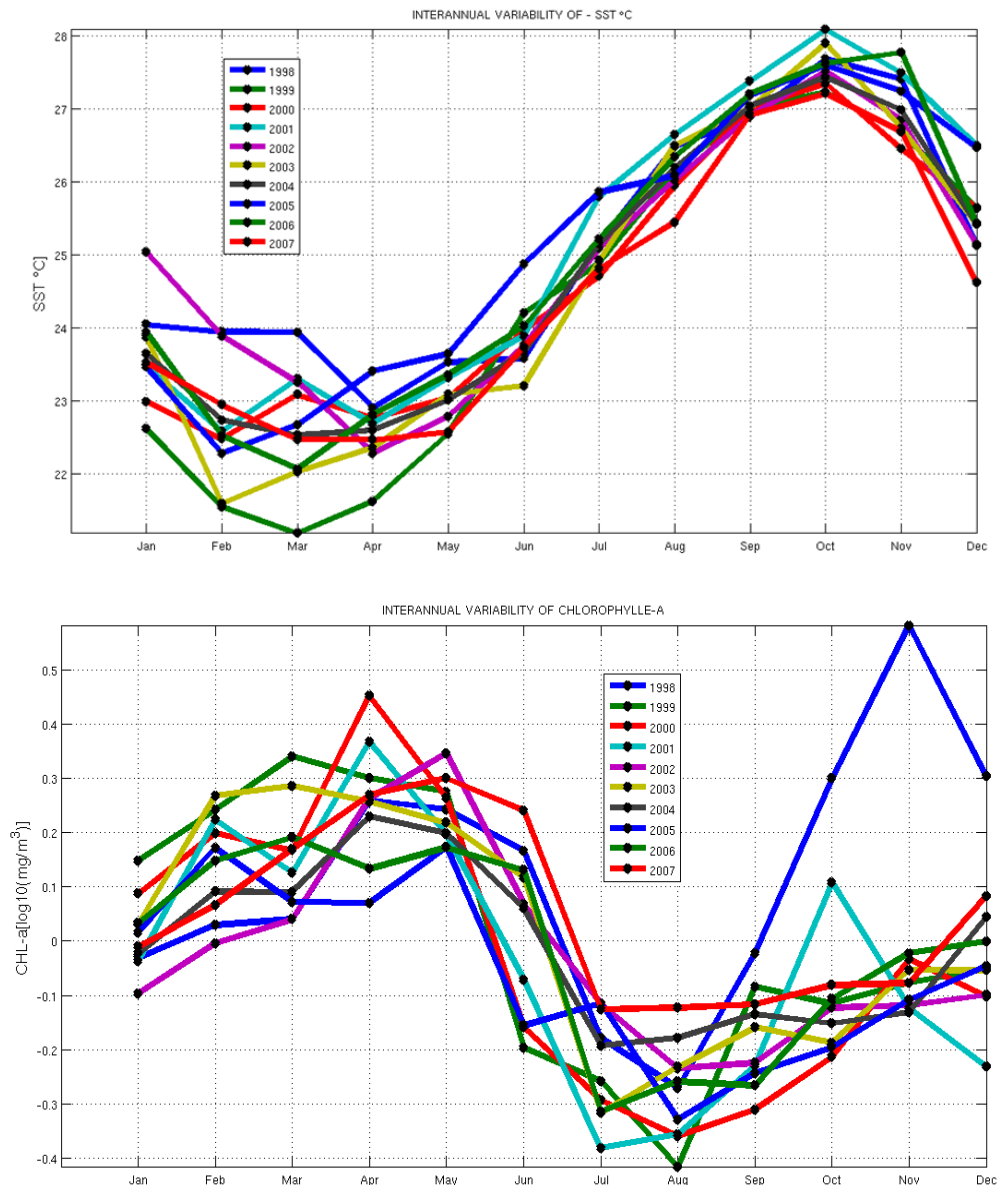
Fig. 4: Seasonal variability of the SST (upper panel) and chlorophyll-*a* concentration (lower panel) averaged over the studied zone for the different years

view Sensor) satellite radiometer and SST by the NOAA AVHRR instrument (Advanced Very High Resolution Radiometer (http://las.pfeg.noaa.gov/Ocean Watch/). We propose to combine these two variables for obtaining an optimum comprehensive description of the upwelling.

Since the upwelling signature is mainly characterized by the offshore gradient of SST (Fig. 2), we thus decided to add a new variable defined as the difference at a given latitude (since the coast is approximately N-S) between the SST at an observed point and the mean SST in the longitude band 22°-26°W which is an offshore region far away from the influence of the coastal upwelling (Demarcq and Faure, 2000). This new variable, denoted ISST, filters out the

important SST seasonal variations (Fig. 4) due to air-sea interactions and large scale oceanic physical phenomena and permits the enhancement of the local dynamical processes. Due to its large variation range and its distribution (many small values and very few large values), Chl-a was expressed it by its Log_{10} value, which is a quantity widely used by biophysicists. The images we processed extend from 9°N to 21°N and from 14°W to 26°W. As the pixel size of the data files is of the order of 11.1×11.1 km, each image is composed of 121×121 pixels. Each pixel of the upwelling is thus represented by a three dimensional vector *D* [Log_{10} (Chl-a), SST and ISST]. In order to overcome the problem of missing data due to clouds or to processing artifacts, which are major problems in

ocean remote sensing, we only considered, for the learning data set, monthly averaged images provided by the NOAA/SeaWiFs site. The learning dataset *D* was built up by averaging the monthly means for the 10 years of observations in order to decrease the number of missing pixels for each month. To reduce the size of the learning data set, we sampled one line out of three of the monthly satellite image matrix. The learning set *D* represents a mean climatology of the behavior of the upwelling for the 10 years under study. After removing the effect land and clouds, *D* consisted of 23893 three-dimensional vectors.

We now present the method we used.

THE METHODOLOGY

We first applied an unsupervised classification similar to that done by Niang *et al*. (2003, 2006). The aim was to summarize the information contained in the three-component vector data set *D* by producing a small number of reference vectors (*rv*) that are statistically representative of the data. Each reference vector (*rv*) represents a set of vectors of *D* that have a similar pattern. In the present case, we chose to determine the *rv*s by minimizing some distance between *rv* and the vectors of *D* it represents. To do this, we used a specific neural network model, the so-called topological map, which was first introduced by Kohonen (1982) and fully described in Kohonen (2001). Each neuron of the map (Fig. 5) is associated with a particular reference vector (*rv*) and thus corresponds to a group (in this study, a set of pixels belonging to *D*). The *rv*s approximate the density of the data set *D*. They are computed by minimizing a specific cost function as in the *K*-Means algorithm (Badran *et al*., 2005). Besides the different neurons of the topological map C are connected together and determine a topological (neighborhood) relationship among the different groups (neurons). Close neurons on the maps correspond to *rv*s that are quite similar; very distant neurons correspond to *rv*s that are very different. The set of *rv*s represents the dataset *D* by compressing the information contained in it.

In the present study, we dealt with a two-dimensional map with quite a large number of neurons (20×20) and therefore of *rv*s, providing a highly discriminating representation of the observations. The pixels of the data set *D* are thus clustered into 400 groups. We used the SOM version available on the web site http://www.cis.hut.fi/projects/somtoolbox/ download/. The topological map was learned according to the procedure described in Niang *et al*. (2003, 2006). The number of neurons was determined empirically from solutions of similar problems and then adjusted as described in Badran *et al*. (2005).

The large number of groups allowed us to take into account the complexity of the dataset but may have prevented us from synthesizing some geophysical information embedded in the data, such as spatial or seasonal specificities. To counteract this difficulty, we
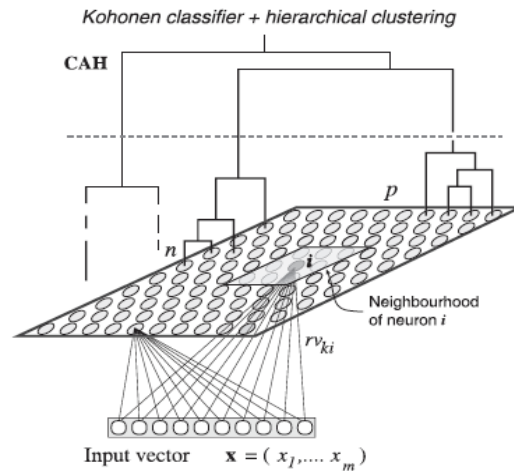

Fig. 5: Structure of the Self-Organizing Map (SOM). The network comprises two layers: an input layer used to present observations and an adaptation layer for which a neighbourhood system is defined. Each neuron i is fully connected to the input layer. It is associated with a group that is represented by a reference vector rvi. In the figure, the neurons are cluster in 3 classes by HAC

decided to aggregate this large number of groups into a smaller number of classes based on the similarities of the groups. We therefore extracted a few pertinent classes from the groups by clustering groups having similar statistical properties, expecting that the classes could be associated with geophysical characteristics. For that we used a hierarchical ascendant classification (HAC in the following), which is a bottom-up hierarchical classification (Jain and Dubes, 1998). This method iteratively computes a partition hierarchy (Badran *et al*., 2005). From the initial partition (the neurons on the map), two subsets of the computed partition are clustered at each iteration. These two subsets are selected by measuring their similarity according to the Ward criterion (Fig. 5).

We aggregated the 20×20 neurons into six significant classes. The resulting clustering of the three-dimension vectors *rv*s associated with the neurons of the topological map is given in Fig. 6. We note that the topological map+HAC clustering is very coherent, since the classes represent clusters whose neurons are contiguous on the topological map. Moreover, the geophysical parameters (SST, ISST and chl-*a*) associated with each neuron (or *rv*) determine homogeneous fields on the SOM. Their gradients are smooth, well defined without any discontinuity. As an example, the chlorophyll-*a* concentration is maximum in the bottom right corner, minimum in the upper left corner of the SOM, the SST is minimum at the bottom, maximum at the top of the SOM. The number of groups (six) was selected because it presented the most significant discriminative partition with respect to the full dendrogram of the HAC (not shown) one the one hand and to the upwelling parameters, on the other hand.
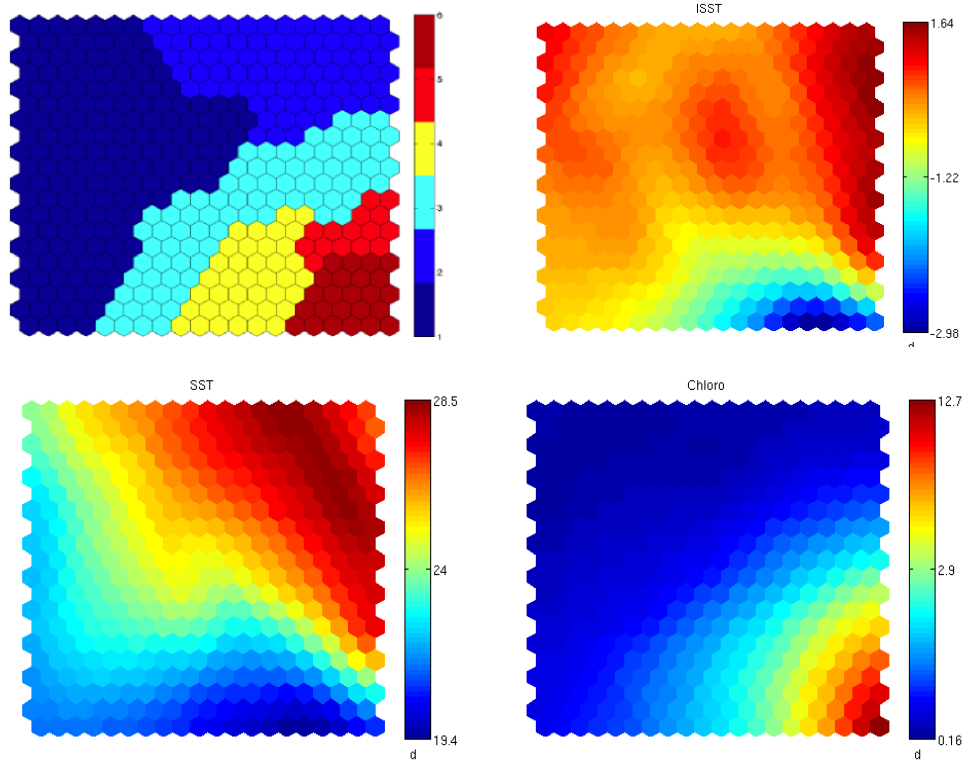
Fig. 6: Upper left panel: Representation of the SOM map clustering in six different classes. Bottom left panel: projection on SOM of SST; the coldest temperatures are in the bottom and highest ones in the upper right side of the map; Upper right panel, projection of the ISST; the coldest ISST are in the bottom right corner and the smallest ones in the upper right side of the map. Bottom right panel: Chlorophyll-*a* concentration; the highest chlorophyll-*a* concentration are located in the bottom right corner of the map, the smallest in the upper left corner of the map
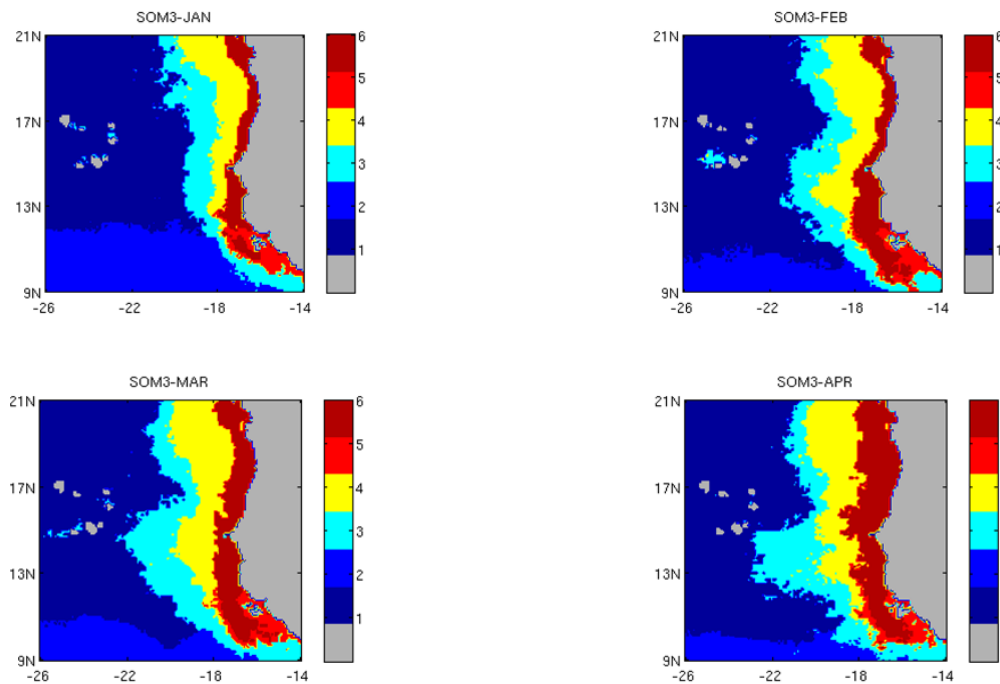

Fig. 7a: Geographical extend of the six classes for January, February, March and April. The classes are identified by the color bars on the right side of the cartoons
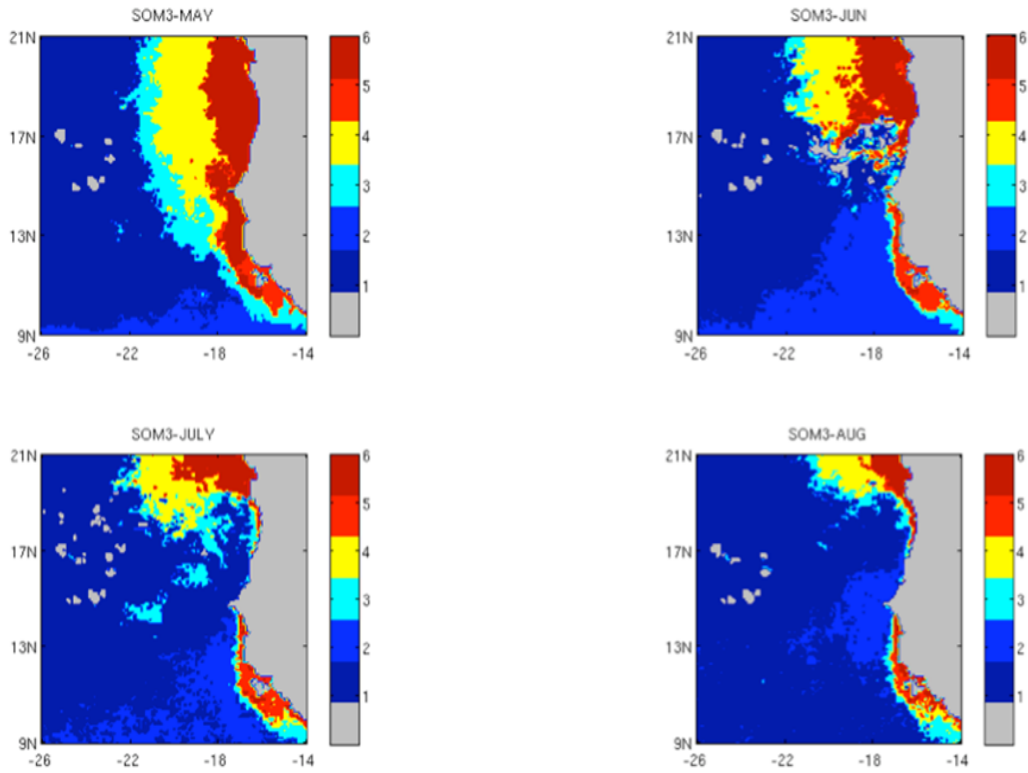
Fig. 7b: Geographical extend of the six classes for May, June, July and August. The classes are identified by the colors bars on the right side of the cartoons
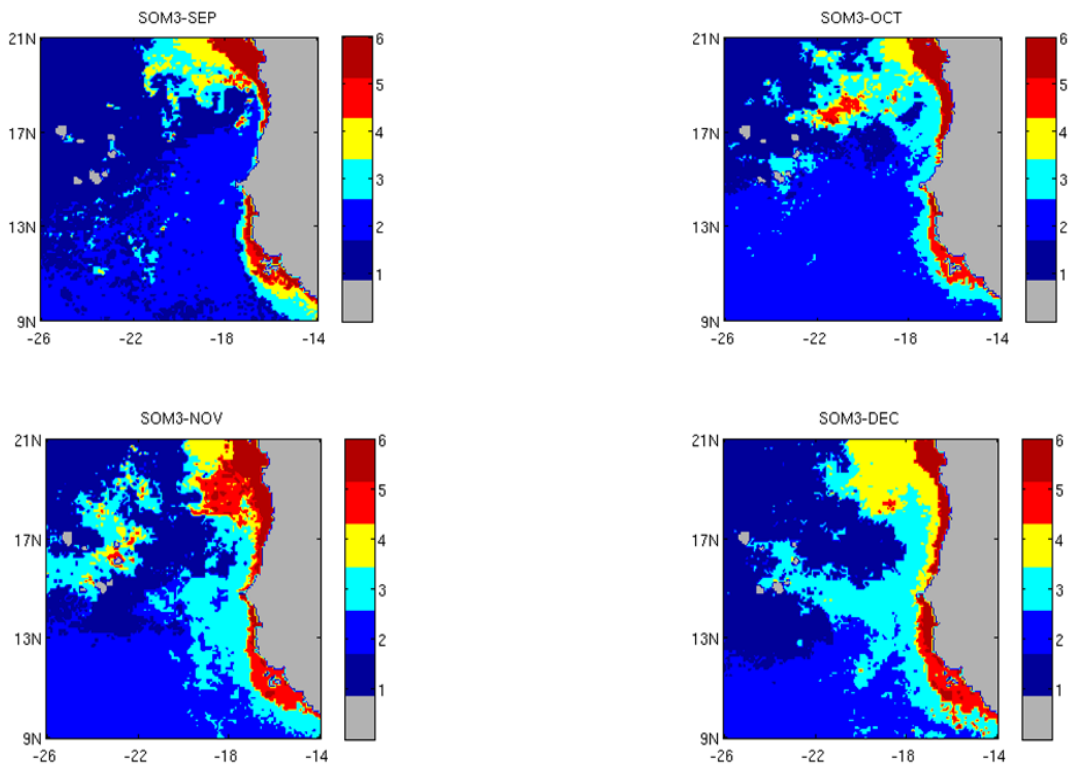

Fig. 7c: Geographical extent of the six classes for September, October, November and December. The classes are identified by the color bars on the right side of the cartoons

ANALYSIS OF THE SIX CLASSES

In the following, we present the mean geophysical characteristics of the six classes for the ten year period we analyzed. Each neuron of the topological map has captured a set of pixels of *D*. We project the set of pixels corresponding to each class for a specific month of the monthly climatology on a geographical map of the studied region (Fig. 7). We observe that the six classes are geographically very coherent, since the pixels of a class are contiguous on the geographical map (Fig. 7). The classes, which have common statistical properties, are then associated with well-defined geographical areas. In Fig. 8, we have displayed the median chlorophyll-*a* content, the median ISST and SST values with their variances associated with the six classes in winter (January), when the upwelling is well developed and in August, when the
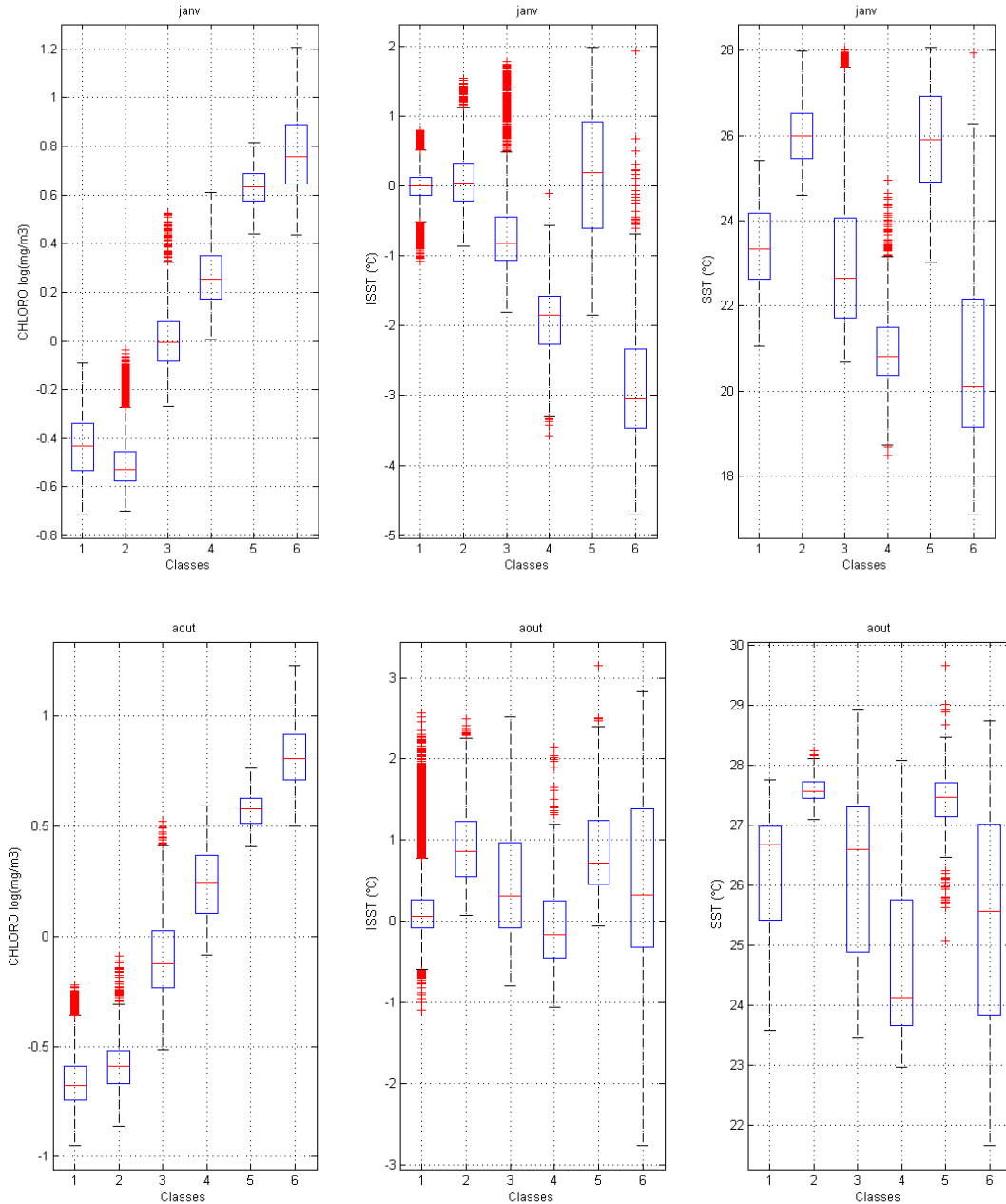
Fig. 8: Chlorophyll-*a* concentration (left hand panels), ISST (middle panels) and SST (right hand panels) values for the different classes in January (top) and August (bottom); Chlorophyll-*a* concentrations are given on a log scale; The little boxes on each panels includes 50% of the pixel values of the dedicated class and the line inside the box represents the median value of the class; The bars outside of each box correspond to the range of the remaining 50%
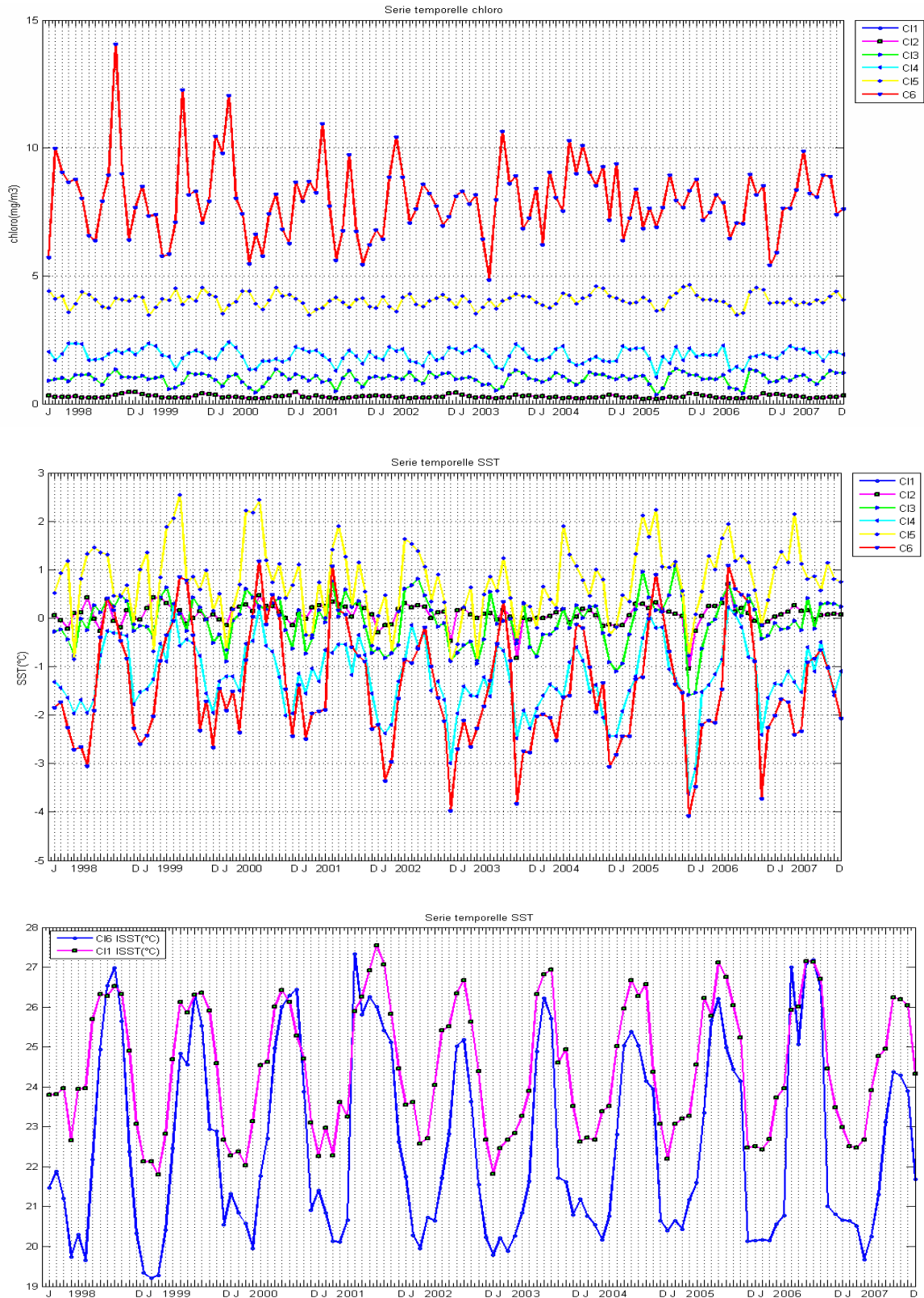
Fig. 9: Times series of the ocean parameters associated with each class: (upper panel) chlorophyll-*a* concentration, (middle panel) ISST, (bottom panel) SST (shown only for class 1 and 6). Note the strong seasonal variability for SST and ISST and chlorphyll-*a* concentration for class 6. The coldest SST were observed in 1999

upwelling signature is the weakest and practically non-existent. We first analyze the six classes from their Chl-a, ISST and SST characteristics:

Class-1: Corresponds to low chlorophyll-*a* concentration and warm SST. Its ISST is close to zero by construction.
Class-2: Corresponds to low chlorophyll-*a* concentration and slightly warmer SST and positive ISST.
Class-3: Corresponds to slightly higher chlorophyll-*a* concentration and slightly colder SST and negative ISST.
Class-4: Corresponds to higher chlorophyll-*a* concentration and cold SST and negative ISST.
Class-5: Corresponds to much higher chlorophyll-*a* concentration and quite warm SST and positive ISST.
Class-6: Corresponds to the highest chlorophyll-*a* concentration and the coldest SST and very high negative ISST.

Similar behavior is observed for the other months.

Figure 7 shows that class-1 (deep blue in the figure) is associated with offshore surface waters unaffected by coastal upwelling. This class extends far from the coast and is associated with a large number of neurons of the topological map (Fig. 6) corresponding to subtle differences in offshore water characteristics.

Due to their geographical location (Fig. 7) and ocean characteristics (Fig. 8) class-3, class-4 and class-6 are associated with the coastal upwelling. Class-6 (deep red in Fig. 7), represents costal upwelling waters with cold temperatures and very high Chl-a concentration. This class is concentrated along the coast and extends a few tens of kilometers offshore. It follows the coast north of Cap Verde (15°N) where the continental shelf is narrow and extends over the Guinea coastal shelf south of 15°N. It is well marked during the boreal winter (January, February, March), for which it can extend down to 12 N and disappears in summer (July, August, September) south of 17°N. Class-4 (yellow in Fig. 7) and class-3 (light blue in Fig. 7) extend quite far offshore. They correspond to waters that have been influenced by the costal upwelling through oceanic processes as instabilities and filaments. Class-3 waters are bounded by class-1 waters at its western limit (Fig. 7). Its offshore extent is important in winter and quite non-existent in summer.

Class-5 (light red in Fig. 7) corresponds to waters rich in chlorophyll and whose temperature is high. These waters are mainly located in shallow water area, such as the Guinea shelf south of 15°N and the Arguin bank at 21°N). The class-5 signature is visible up to 19°N in July, August and September replacing Class-6 waters at some location south of that latitude. In winter (January to April), class-5 waters (light red in Fig. 7)

are confined South of 12°N in the coastal region, covering the shallow continental Guinea shelf shown in Fig. 1. In fact, these waters are suspected to correspond to case-2 waters, which are coastal waters for which Chl-a, sediments and dissolved maters are mixed, leading to an overestimation of chlorophyll-*a* concentration values due to absorption of incoming solar radiation by the dissolved maters.

Class-2 waters (sky blue in Fig. 7) are waters whose chlorophyll-*a* concentration is quite small and temperature warm. They are located in the south part of the region during winter and spring. They move northward at the beginning of summer and reach 17°N in September, staying at that latitude until October and then moving back to south at the end of November. These waters may represent a signature of the North Atlantic Equatorial Counter Current (NECC), which intensifies in summer and forms the so-called Guinea Dome (Siedler *et al*., 1992). During their northward progression in summer, class-2 waters never invade the Guinea continental shelf, which is mainly covered with class-5 and class 6 waters.

The SST of the six classes presents a well-marked seasonal variation, which is shown in (Fig. 8) and on monthly mean SST time series (Fig. 9). The SSTs of the six classes vary in phase. The SST is maximum in October and minimum in February-March-April. The seasonal variation is associated with the seasonal variation of the long shore component of the wind, which generates an offshore Ekman transport and thus a mass deficit, which is compensated by an upward advection of deep cold waters rich in nutriment at the coast. Surprisingly the chlorophyll concentration does not show well-marked seasonal variation as seen in Fig. 9, except for class 6, whose Chl-a values present high seasonal and inter annual variations during the first five years of the studied period which could not be related to any identifiable indices such as NAO, Enso or African monsoon indices.
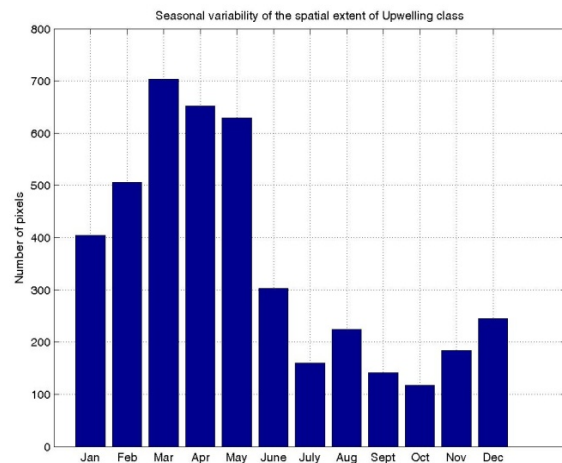

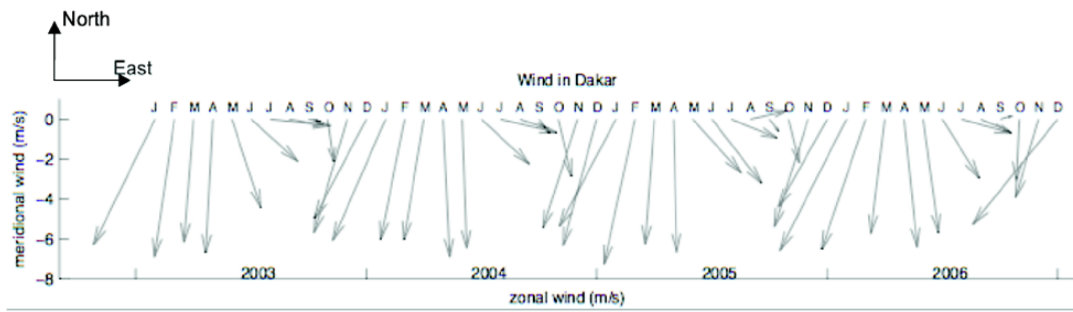Fig. 10: Seasonal variability of the spatial extent of class 6 waters

Fig. 11: Time series of the monthly wind vector at Dakar from 2003 to 2006. The wind direction is given according to the axes drown in the upper left panel

Moreover, we note that the extent of class 6 waters, which is associated with the coastal upwelling, presents a strong seasonal variation as shown in Fig. 10. This extent is minimum in summer (July to September). It starts to grow in November, is maximum in March, stays well developed until May and begins to decrease in June. This extent is associated with the long shore component of the trade winds. The decrease is linked to the northward progression of the ITCZ (Inter Tropical Convergence Zone) and the ensuing decrease in intensity of the trade winds that drive the upwelling dynamics (Fig. 11). The ratio between the maximum extent class-6 area and its minimum extent is about 6, showing the strong variability of the upwelling area.

In Fig. 11 shows the time series of the monthly wind vector at Dakar from 2003 to 2006. The wind presents a strong seasonal variability, with a maximum in winter (November to May) and a minimum in summer (July, August, September) when the ITCZ reaches its northernmost position. We note that the seasonal variability of the extent of class 6 waters shown in Fig. 10 varies with the southward component of the wind, in agreement with the upwelling theory (Allen, 1973). The more intense the North South wind component, the larger the extent of class 6 waters.

CONCLUSION

A Self Organizing Map (SOM) associated with a hierarchical ascending clustering provides an efficient index to investigate the variability of the Senegalo-Mauritanian upwelling by combining SST, ISST and chlorophyll-*a* values observed by satellite remote sensors using a multivariate statistical relationship. The grouping of the data in few (six) classes based on three major signatures of the upwelling, SST and ISST, as physical parameters and chlorophyll-*a* concentration as biogeochemical parameter, allowed us to study the variability of the upwelling. This method has enabled us to pick up the major characteristics of the Senegalo-Mauritanian upwelling. The values of the upwelling parameters are very distinct for the six classes (Fig. 9) justifying the CAH classification a posteriori. In Fig. 6,

we have displayed the decomposition in six classes on SOM and in Fig. 7 the geographical pattern of the six classes. The different classes can be related to ocean phenomena: class 6 corresponds costal upwelling waters (cold and high Chl-a concentration), while class 1 corresponds to offshore waters (warm and low Chl-a concentration). Class 4 and 3 correspond to waters, which have been influenced by the upwelling through temperature and chlorophyll-*a* diffusion due to filaments and instabilities. Class 2 can be related to the NECC waters moving northward in June-July with the ITCZ displacement and enhancing the dome of the Gulf of Guinea. Class 5 can be associated with shallow shelf waters corresponding to class-2 water. It mainly corresponds to case-2 waters and is found on the Arguin bank and on the shallow shelf extending off the Gambia and Guinea coasts. This was confirm by analyzing the nLw* spectrum (spectrum normalized by the Chl-a spectrum). The class 5 normalized spectra are always larger than unity, which could be due to the effect of the light backscattering onto the sediment particles present in the waters, confirming that these waters are case-2 waters. The class 6 normalized spectra, which are also larger than unity can interpreted by high chlorophyll-*a* concentration associated with a large variety of phytoplankton species. This may lead to an important package effect (Bricaud *et al.*,) that makes the chlorophyll-*a* concentration-absorption relationship non-linear and the normalized spectrum different from unity. The very high variance for classes-5 and -6 indicates the complexity of the interaction between the incoming solar radiation and the biogeochemical constituents of the water column.

Our method has also enabled us to quantify the spatial extent of the upwelling in terms of pixel numbers and estimate its seasonal variability. The variability of this extent is linked to the variability of the southward component of the wind that is parallel to the coast. Nevertheless, for the ten years of observations, we were not able to detect any climatic trends in the SST of the different classes, nor in the chlorophyll-*a* concentration. This might be due than in strong upwelling area as fed by deep waters, the

characteristics of this deep water are much more stable than surface layers. Moreover, despite attempting to investigate the inter-annual variability of the upwelling in terms of spatial extent and duration (expressed in month of the year) in respect of class 6, which reflects the upwelling dynamics, we were not able to reach definite conclusions regarding the inter annual variability of this extent, which is quite small and is biased by the cloud coverage masking the relaxation of the upwelling in summer and very often its spatial extent all year around. This effect is important during the summer months (July, August, September), leading to spurious effect on the class extent.

The results of the method we have developed show the interest in combining the different variables through a unique multivariate statistical process rather than to combine the results of analysis done separately on the different variables. As an example, analysis of the chlorophyll-*a* concentration can provide classes having similar concentration; analysis of ISSTs or SSTs can also provide classes having similar ISSTs or SSTs. But the merging of three contours obtained separately is a very delicate operation whereas the multivariate analysis done by SOM provides an optimum combination of the information embedded in the three data sets. Class 5 and class 2 oceanic characteristics would not have been easily identified by applying mono variable statistical methods on each variable separately.

The method we have presented is relevant to analyze a large variety of phenomena, which have been observed with several different sensors. It permits to combine different measurements given by different sensors in a rational manner to extract pertinent information on the phenomena, which would not have been obtained by using the observation separately as shown in this study. Moreover, the present method, which uses SOM, is very easy to implement and to handle, as there exists friendly software dedicated to the handling them. Other method such as k-means could also be used to make data fusion analyses. In fact, SOM is an extension of the K-means method in which the different clusters are related together allowing a more efficient partitioning as shown in Badran *et al.*, 2005), especially when the analyzed data set is related to complex physical laws.

ACKNOWLEDGMENT

REFERENCES

Allen, J.S., 1973. Upwelling and coastal jets in a continuously stratified ocean. J. Phys. Oceanogr., 3(3): 245-257.

Aristegui, J., X.A. Alvarez-Salgado, E.D. Barton, F.G. Figueiras, S. Hernandez-Leon, C. Roy and A.M.P. Santos, 2004. Oceanography and Fisheries of the Canary Current/Iberian Region of the Eastern North Atlantic. In: A.R. Robinson and K.H. Brink (Eds.), the Sea. Chapter 23, John Wiley and Sons Inc., New York, 14: 877-931.

Badran, F., M. Yacoub and S. Thiria, 2005. Self-organizing Maps and Unsupervised Classification. In: Dreyfus, G. (Ed.), Neural Networks, Methodology and Applications. Chapter 7, Springer, Berlin, Heidelberg, New York, pp: 379-442.

Barth, J.A., 1989. Stability of a coastal upwelling front 2. Model results and comparison with observations. J. Geophys. Res., 94(C8): 10844-10856.

Barton, Eastern Boundary of the North Atlantic, 1998. Northwest Africa and Iberia. In: Robinson, A.R. and K.H. Brin (Eds.), the Sea. John Wiley and Sons Inc., New York, 11: 633-657.

Beletsky, D., W.P. O'Connor, D.J. Schwab and D.E. Dietrich, 1997. Numerical simulation of internal Kelvin waves and coastal upwelling fronts. J. Phys. Oceanogr., 27: 1197-1215.

Bricaud, A., A. Morel and J.M. André, 1987. Spatial/temporal variability of algal biomass in the Mauritanian upwelling zone, as estimated from CZCS data. Adv. Space Res., 7(2): 5362-5384.

Brink, K., 2005. Coastal Physical Processes Overview. In: Robinson, A. and K. Brink (Eds.), Harvard University Press, NY.

Crepon, M., C. Richez and M. Chartier, 1984. Effect of coastline geometry on upwellings.J. Phys. Oceanogr., 14(8): 1365-1382.

Demarcq, H. and V. Faure, 2000. Coastal upwelling and associated retention indices from satellite SST. Application to octopus vulgaris recruitment. Oceano. Acta, 23: 391-407.

Jain, A.K. and R.C. Dubes, 1988. Algorithms for Clustering Data. Prentice Hall, Englewood, Cliffs, New Jersey, pp: 320.

Kohonen, T., 1982. Self-organized formation of topologically correct feature maps. Biol. Cybernet., 43: 59-69.

Kohonen, T., 2001. Self-Organizing Maps. 3rd Edn., Springer, Berlin, Heidelberg, New York.

Lachkar, Z. and N. Gruber, 2012. A comparative study of biological production in eastern boundary upwelling systems using an artificial neural network. Biogeosciences, 9: 293-308.

Lange, C.B., O.E. Romero, G. Wefer and A.J. Gabric, 1998. Offshore influence of coastal upwelling off Mauritania, NW Africa, as recorded by diatoms in sediment traps at 2195 m water depth. Deep Sea Res. I, 45: 985-1013.

Lathuiliere, C., V. Echevin and M. Levy, 2008. Seasonal and intraseasonal surface chlorophyll-a variability along the northwest African coast. J. Geophys. Res., 113: C05007.

Niang, A., L. Gross, S. Thiria, F. Badran and C. Moulin, 2003. Automatic neural classification of ocean colour reflectance spectra at the top of atmosphere with introduction of expert knowledge. Remote Sens. Env., 86(2): 257-271.

Niang, A., F. Badran, C. Moulin, M. Crépon and S. Thiria, 2006. Retrieval of aerosol type and optical thickness over the Mediterranean from SeaWiFS images using an automatic neural classification method. Remote Sens. Env., 100(15): 82-94.

O'Brien, J.J. and H.E. Hurlburt, 1972. A numerical model of coastal upwelling. J. Phys. Oceanogr., 2(1): 14-26.

Siedler, G., N. Zangenberg, R. Onken and A. Morlière, 1992. Seasonal changes in the tropical atlantic circulation: Observation and simulation of the guinea dome. J. Geophys. Res., 97(C1):703-715.